IPTEK The Journal of Technology and Science, 35(1), 2024 (e/pISSN:2088-2033, 0853-4098)

DOI: 10.12962/j20882033.v35i1.16852 | Received 23 May, 2023; Revised 8 Aug, 2023; Accepted 24 Jan 2024

ORIGINAL RESEARCH

FUNCTIONALIZATION OF CARBON NANOTUBES AS SUPPORT MATERIAL OF Pt/CNTs CATALYST FOR PROTON-EXCHANGE MEMBRANE FUEL CELL

Agung Purniawan*[1] | Lukman Noerochim[1] | Sutarsis[1] | Haryo Satriya Oktaviano[2] | Hafidz Alim Sukmana[1] | Muhamad Akbar Wicaksono[1] | Berlian Aulia Rachman[1] | Wikan Jatimurti[1] | Diah Susanti[1] | Hanifudin Nurdiansyah[1] | Muhammad Fakhreza Abdul[1]

[1]Departement of Material and Metallurgical Engineering, , Institut Teknologi Sepuluh Nopember, Surabaya 60111, Indonesia

[2]Downstream Research and Technology Innovation, Innovation and New Ventures, PT Pertamina (Persero), Jakarta 10110, Indonesia

Correspondence

*Agung Purniawan, Dept of Material and Metallurgical Engineering, Institut Teknologi Sepuluh Nopember, Surabaya, Indonesia.
Email: agung_pur@mat-eng.its.ac.id

Present Address

Department of Material and Metallurgical Engineering, Institut Teknologi Sepuluh Nopember, Surabaya, 6011, Indonesia

Abstract

The Proton Exchange Membrane Fuel Cell (PEMFC) is a type of fuel cell that converts hydrogen fuel into electrical energy. In PEMFC, platinum (Pt) supported by carbon black (CB) is frequently used as a catalyst. The catalyst has several constraints cause it to agglomerate and corrode during fuel cell operations. Carbon Nanotubes (CNTs) are a contender as a catalyst-supporting material because they offer superior properties such as hydrophobicity, conductivity, and surface area. This study used pH modifications in the synthesis process, morphology, and electrochemical performance of the Pt/CNTs catalyst to evaluate the reduced size of Pt particles and increased CNTs surface area. During the catalyst synthesis procedure, colloidal solutions with pH variations of 11 and 13 were utilized. TEM analysis showed that at pH 13, the produced Pt nanoparticles had the least average particle size of 4.2 nm, followed by 5.1 and 7.9 for pH 9 and 11, respectively. The best electrochemical performance was achieved in pH 13 samples with the largest active surface area of 40.33 m2/g, an onset potential of 0.798 V involving 4.01 electrons for the oxygen reduction reaction, and the lowest risk of deterioration.

KEYWORDS:

Carbon Nanotube (CNT), Catalyst, Fuel Cell, PEMFC

1 | INTRODUCTION

Climate change induced by fossil fuels is accelerating the transition from fossil fuels to renewable energy sources (RER) to reduce carbon emissions. The use of fossil fuels has resulted in their depletion[1]. Recently, a technique known as Fuel Cell

technology has been recognized as a promising technology alternative for power generation. A Fuel Cell is an electrochemical system that directly transforms chemical energy from hydrogen and oxygen into electrical energy. Among all fuel cell types, the Proton Exchange Membrane Fuel Cell (PEMFC) is a promising device for producing portable energy [2].

To substitute for conventional energy sources, fuel cell performance and durability must be improved, as well as fuel cell costs. Catalytic support materials can be improved to reduce the amount of Pt, lowering the cost. Carbon black (CB) is frequently utilized as a catalytic support material. However, CB's amorphous structure tends to deteriorate, limit the service life of fuel cells, or reduce their effectiveness [3]. According to the literature, surface modification and morphology of catalyst support materials, particularly carbon-based materials, can influence the nature of PEMFC catalysts [4].

Among the numerous forms of carbon, carbon nanotubes (CNTs) are known for their great structural homogeneity and electrical conductivity, as well as their high surface area, high thermal conductivity, extraordinary strength, and durability [3]. When utilized correctly, this property has been shown to improve the performance of fuel cell catalysts. A Fuel Cell is an 'electrochemical' device that converts chemical energy or combustion heat from fuel (e.g., hydrogen, methanol, etc.) and oxidants (e.g., air or pure oxygen) into electricity using catalysts [2]. The operational fuels and electrolytes used in fuel cells, notably the Proton Exchange Membrane Fuel Cell (PEMFC), are classified.

Unlike most other forms of fuel cells, PEMFC uses electrolytes consisting of polymers with acid-based clusters on their side chains to generate electricity, water, and heat from hydrogen and oxygen gases in the air. PEMFC features include low-temperature operation (below 90°C), high power density, a compact system, and ease of handling gas fuel [5]. In PEMFC, chemical energy is converted into electrical energy via direct electrochemical processes. The flow channel transports hydrogen to the anode. The cathode receives oxygen from the free air on the other side of the cell. [6]

The Hydrogen Oxidation Reaction (HOR) happens in anodes, with hydrogen depicted as a positively charged proton and negatively charged electrons in Equation 1 [7]:

$$H_2 \rightarrow 2H^+ + 2e^- \tag{1}$$

Positively charged protons flow through the Polymer Electrolyte Membrane (PEM) to the cathode, while negatively charged electrons flow through the external circuit, providing an electric current. In the cathode, there is an Oxygen Reduction Reaction (ORR) in which electrons meet protons and, along with oxygen molecules, form clean water as the only consequence of the reaction, as shown in Equation 2. [7]

$$\frac{1}{2}O_2 + 2H^+ + 2e^- \rightarrow H_2O \tag{2}$$

The total electrochemical reaction is as follows:

$$H_2 + \frac{1}{2}O_2 \rightarrow H_2O \tag{3}$$

A variety of factors can affect the performance and durability of Pt catalysts. The size and dispersion of Pt particles in the catalytic support are two of the most important parameters. Many previous investigations have revealed that the ideal Pt particle size is 3-5 nm. The graph shows that (i) mass activity reaches a maximum of roughly 3-5 nm and (ii) mass activity increases as particle size decreases. Pt (iii) specific activity diminishes as particle size decreases Pt [8]. CNTs are two-dimensional nanostructures typically created by rolling a single sheet of hexagonally put-together carbon atoms or graphene. CNTs are divided into two types, i.e., single-walled nanotubes (SWNT) and multi-walled nanotubes (MWNT). Single-walled nanotubes (SWCNT) have numerous forms, including armchair zigzag and chiral, as shown in Figure 5 . (A). MWCNT is a structure composed of many layers of graphene rolled into a concentric cylindrical form with a constant interlayer separation of 0.34 nm. MWCNT has a wider diameter, ranging from a few nanometers to dozens of nanometers, and so serves as a better delivery material [5]. CNT offers a higher surface area and electronic conductivity than typical carbon black for Pt catalyst support, both favored for their usefulness as electrocatalyst supports.

2 | PREVIOUS RESEARCH

CNT materials are more resistant to electrochemical oxidation than carbon black, which is extensively used today.[9] Because CNTs have a more contained structure than carbon black, they are more resistant to breakdown in oxidative circumstances.[10] Because CNT material products are often inert and hydrophobic, platinum deposition on their surfaces is not appropriate. As a result, hydrophilic functional groups in the form of hydroxyl groups containing oxygen must be added to the surface of the CNT, a process known as functionalization. The wet oxidation approach can add functional groups to CNTs by utilizing chemicals as oxidizing agents (acids and potent oxidizers)[11]. The formation of flaws on the surface of carbon nanotubes due to acid oxidation produces alkyl (CHn). Further oxidation will result in the formation of alcohol (-OH), followed by C=O, and finally, functional groups such as carboxyl, carbonyl, and phenolic can react with other groups. Deposing Pt nanoparticles into CNT is another critical stage in the catalyst synthesis technique. When Pt ions are added to the synthesis solution, they interact with and bind to the surfaces of carbon function groups such as carboxyl, carbonyl, and phenolic via ion exchange processes, serving as nucleation precursors. After reducing surface Pt precursor ions with hydrogen ions, well-dispersed Pt metal nanoparticle deposition on the surface of CNT is produced[12].

A technique of synthesis based on liquid-phase precursors is recommended for metal nanoparticle precursor reduction because it allows for particle size control. Colloidal methods include the production of pre-reduction metal particles, which are then dissolved or kept in catalyst support. The advantage of this approach is that colloidal chemistry determines particle size, resulting in a catalyst with a narrow particle size distribution. The main disadvantage is the presence of stabilizing chemicals, which might decrease the catalytic efficiency of catalyst nanoparticles. Recent research has demonstrated that Ethylene Glycol (EG) can be utilized as both a stabilizer and a reduction. At high temperatures, EG breaks down to produce acetate, which is thought to decrease and stabilize metal colloids. There is no need for additional stabilizers in this situation, and it is recommended that the metal be linked to the active surface of the CNT first and then stabilized with Ethylene Glycol (EG). The reaction mechanism of the addition of Pt nanoparticles in CNT with EG solution reduction is described in greater detail in (a) the overall mechanism, the shift from pure (I) to oxygen (II) to decorating Pt (III), and (b) the attachment and production of Pt nanoparticles[3].

In this study, the pH of the Pt/CNT catalyst synthesis reaction environment was varied using colloidal methods to examine the effect of these parameters on the phase, morphological form, and electrocatalytic performance of Pt/CNT for proton exchange membrane fuel cell (PEMFC) applications. The findings are expected to serve as a reference in defining the next technique for synthesizing PEMFC catalysts and to provide recommendations for future PEMFC catalyst research and development.

3 | METHOD

The functionalization of MWCNT with acid treatment is the first step in developing Pt/CNT catalysts. Using MWCNT from Times Nano, China, with a diameter of 8–15 nm, a length of 50 m, a purity of >95%, and a surface area of more than 140 m2/g The first step is to functionalize MWCNT with H2SO4/HNO3 at a concentration of 65%/97% and a ratio of 3:1 (%v). SAP Chemicals provided H2SO4 solution (98% PA), HNO3 (65% PA), NaOH, aquabides, and EG. 1 gram of MWCNT is weighed with a digital scale and ultrasonically dissolved in a beaker glass with 100 ml (approximately 3.38 oz) of H2SO4/HNO3 combination for 1 hour in a water bath. The MWCNT solution dispersed in the H2SO4/HNO3 mixture was then oxidized at $100^{o}C$ in reflux conditions for 6 hours.

Following the completion of the MWCNT functionalization process and the formation of functional at 110 °C carbon nanotubes (FCNT), the filtration and flushing process is carried out, as shown in Figure 8 . The filtration method employs an aqueous rinse up to pH 7 to extract and neutralize FCNT from the rest of the associated mixed solution. This procedure uses vacuum filtration on a Buchner's funnel coated with Whatman filter paper with a diameter of 2.5 m, as shown in Figure 8 . After washing and filtering, dry on the muffle furnace for 12 hours at $110^{o}C$. Furthermore, after drying the FCNT, the examination process uses TGA (Thermogravimetric Analysis).

Following the completion of the MWCNT functionalization process and the formation of FCNT, the Pt/CNT synthesis process is carried out utilizing FCNT. Colloidal techniques are used in the synthesis process. First, to create Pt/CNT with a platinum content of 20%, dissolve 160 mg of FCNT in EG in a beaker glass. Separately, 100 mg of H2PtCl6.6H2O is weighed on digital scales and dissolved in EG as a reducing agent for preparing precursor solutions. Smart Lab provided H2PtCl6.6H2O with a Pt

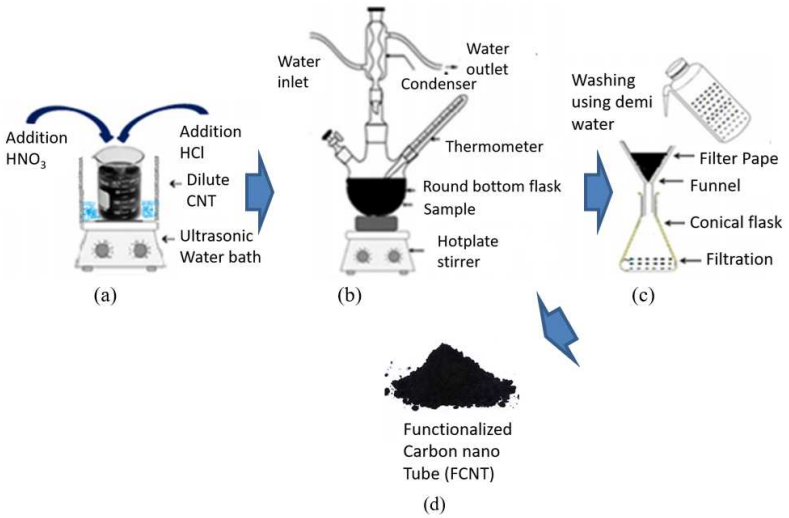

FIGURE 1 MWCNT Functionalization Process Schematic (a) functionalized carbon nanotubes (FCNT) mixing, (b) stirring, (c) filtration, and (d) heating and drying

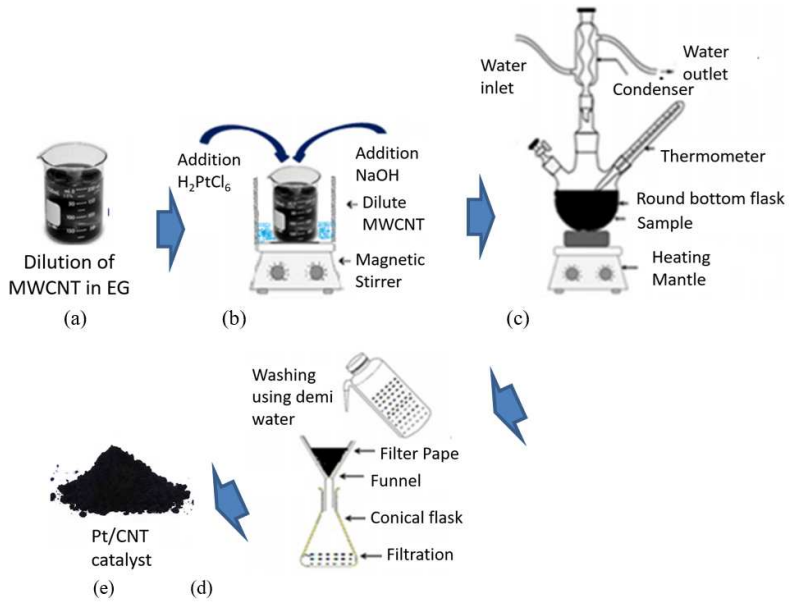

FIGURE 2 Schematic of Pt/CNT catalyst synthesis process (a) dilution process, (b) stirring, (c) heating, (d) filtering, and (d) Pt/CNT catalyst

concentration of 40%. The precursor solution is gradually dripped into the CNT solution for 5 hours while forceful stirring at 450 rpm is done, followed by 3 hours of ultrasonication. As illustrated in Figure 9 , the reaction was carried out in reflux conditions at the base pH of the variables (pH 9, 11, and 13) with the addition of a 0.1 M NaOH solution received from SAP Chemicals in EG. After the synthesis process and the Pt/CNT is created, it is filtered and flushed. The filtration method involves rinsing Pt/CNT with aqueous solutions up to pH 7 to remove and neutralize Pt/CNT from the remaining connected mixed solution. This procedure is carried out using a Buchner funnel coated with filter paper made of nylon with a diameter of 0.4 m and aided by vacuum filtration. After washing and filtering, dry at 70^oC for 8 hours. Furthermore, after getting dried Pt/CNT, the analysis process uses TGA, XRD, TEM, and ORR.

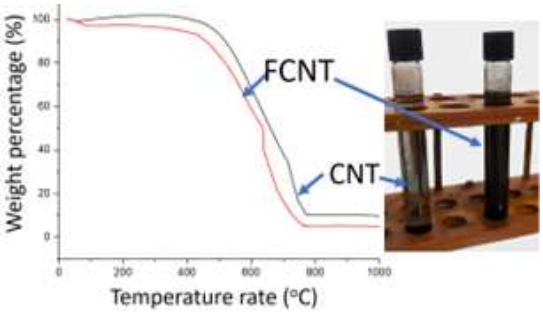

FIGURE 3 TGA and solubility test findings of unfunctionalized CNT versus functionalized CNT (FCNT).

4 | RESULT AND DISCUSSION

TGA characterization is employed to identify the thermal characteristics of a sample's degradation rate due to rising temperatures based on changes in mass percentage. TGA testing is carried out up to 1000^oC. Figure 3 depicts the results of TGA testing on both samples. The link between the temperature curve and the percentage of mass change

The thermal analysis of unfunctionalized CNT and functionalized CNT (FCNT) using TGA is shown in Figure 3 . According to the TGA curve, the temperature at which the mass drop starts differs between CNT and functionalized CNT. At 450^oC, CNT material shows a considerable weight decrease to 780^oC. This shows that carbon is beginning to lose most of its weight, which increases progressively as post-carbonization temperatures rise. Functionalized CNT exhibits a weight loss at a lower temperature of around 430^oC, indicating a faster, more stable combustion line at 760^oC. Faster functionalized CNT initiation temperatures could suggest surface deterioration induced by the oxidizing chemical utilized.

The drop in functionalized mass of CNT below 150°C can be attributed to a decrease in moisture content, which is more prominent. This represents an increase in hydrophilic characteristics following CNT functionalization. Functionalization in CNT has also been shown to reduce the mass of metal residues from impurities produced during CNT synthesis, including Fe metal, ferrocene residue, and benzene residue, which has not been lost until only 4.75% is left compared to CNT, which still has a 9.78% percentage of residual metal residue mass. Figure 3 depicts a solubility test of both samples in water to assess changes in hydrophilic characteristics.

The solubility of functionalized CNT samples rises, and they tend not to separate again. It demonstrates the quality of hydrophilic characteristics following CNT functionalization. This is consistent with the findings, who found that functionalizing CNT with HNO3/H2SO4 caused the development of carboxylic and hydroxyl functional groups along the CNT sidewall. The presence of this functional group reduces the van der Waals force between CNT molecules, allowing CNT to separate and become hydrophilic, allowing for further modification with the solution base. X-ray diffraction (XRD) testing was performed on colloidally produced Pt/CNT catalyst samples with pH variations of 9, 11, and 13. This test was conducted to determine the composition of the catalyst material Pt / CNT synthesis findings with peak XRD indications. It was also used to determine the material's structure to know the content of the phase generated.

Furthermore, XRD data revealed a drop in intensity at the peak of Pt material that is gradually swallowed as pH increases. This demonstrates the tendency of Pt nanoparticle crystals to become amorphous as the pH rises. This amorphous structure can be created by an excessively quick crystallization process, resulting in particles formed from smaller crystals. This claim can be supported further. These findings are similar to prior research on Pt/GO catalyst material production, which found that as the pH of the synthesis conditions increased, the peak intensity of the XRD test of Pt nanoparticles increased.

Using a Transmission Electron Microscope (TEM), the electrocatalytic surface structure of Pt/CNT was studied. Figure 5 depicts the electrocatalytic morphological structure of Pt/CNT at pH 9, pH 11, and pH 13. Furthermore, to validate the hypothesis of the XRD data, Pt particle size was evaluated in the synthesis of catalyst Pt / CNT in reaction conditions at pH 9, pH 11, and pH 13. The findings of particle size calculations using ImageJ software reveal that the average Pt particle size decreases as pH conditions increase. Whereas the crystal Pt in the sample at pH 9 has the biggest average particle size of 7,872 nm and pH 11

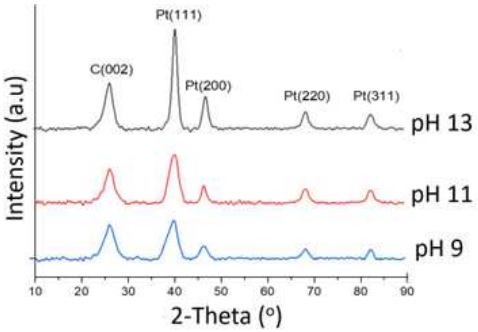

FIGURE 4 XRD characterization of a Pt/CNT catalyst The results of the XRD test shown in Figure 4 exhibited some peak intensity of the material. Based on JCPDS data 00-041-1487, the carbon peak identified in 2 θ was around 26^o, corresponding to the Miller index (002), suggesting the presence of carbon nanotubes. Based on JCPDS 04-0802 data, the other four peaks arise at 2 = 40^o, 46^o, 67^o, and 81^o, corresponding to the Miller index (111), (200), (220), and (311), exhibiting Pt nanoparticles from the breakdown of hexachloroplatinic acid precursors. This well-shaped peak behavior characteristic explains why Pt crystals are face-centered cubic.

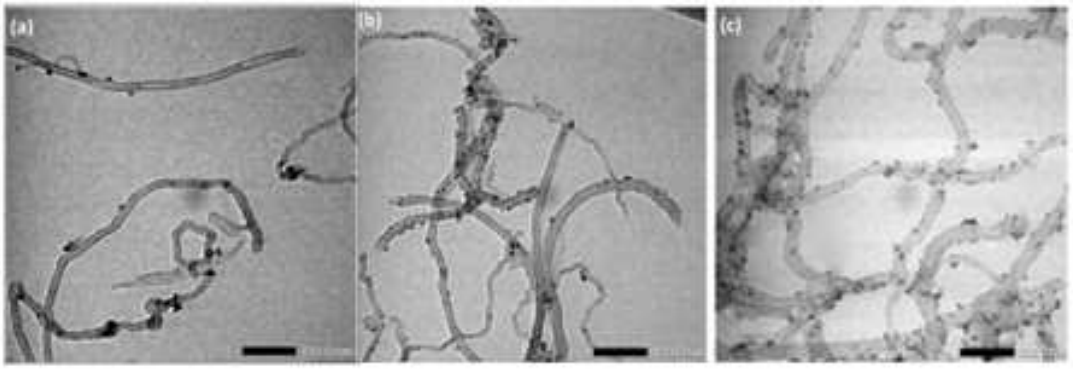

FIGURE 5 TEM images of Pt nanoparticles bound to CNT surfaces at 40,000x magnification (a) at pH 9, (b) at pH 11, and (c) at pH 13.

has the smallest average particle size of 5,096 nm, the Pt particle in the pH reaction condition is greater at pH 13. It has the smallest average particle size of 4,208 nm.

Figure 5 depicts the TEM test findings. Pt nanoparticles are black and connected to the outer surface of the tube-shaped CNT. When observed at a lower pH, nanoparticles Pt are accelerated around the CNT particles in the form of dark deposits, resulting in less equal dispersion of the nanoparticles Pt than when observed at a higher pH. Schrader's research can explain this. The massive quantity of agglomerated Pt particles is due to a shortage of OH- availability required for particle protection during synthesis conditions. When the synthesis situation declines, so does the supply of OH for particle protection. No OH- is left for particle stabilization once all OH- is neutralized by protons generated in equation reaction 2.5. As a result, particles are no longer stable and are ineffectively shielded. Particles will begin to increase in size and cluster together to produce deposits of black particles. As a result, samples created in higher alkalinity settings can produce smaller particle sizes than samples formed in lower alkalinity environments.

As shown in Figure 6 , the electrochemical performance of Pt/CNT as a PEMFC electrocatalyst was investigated using cyclic voltammetry analysis, which offers an overview of performance for the Hydrogen Oxidation Reaction (HOR).

The hydrogen adsorption area from the CV experiment can be used to determine the Electrochemical Surface Area (ECSA), which represents the value of the electrocatalyst's active surface area versus the electrolyte. The calculated active surface area of the catalyst under a pH variation of 13 revealed that the catalyst has an active surface area of 40.33 m2/g. This result was better

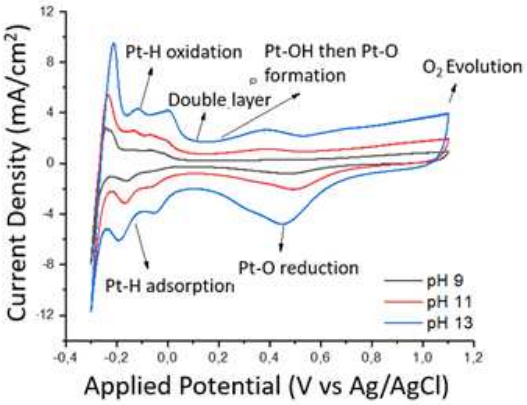

FIGURE 6 Effect of Pt/CNT functionalization on cyclic voltammetry curve

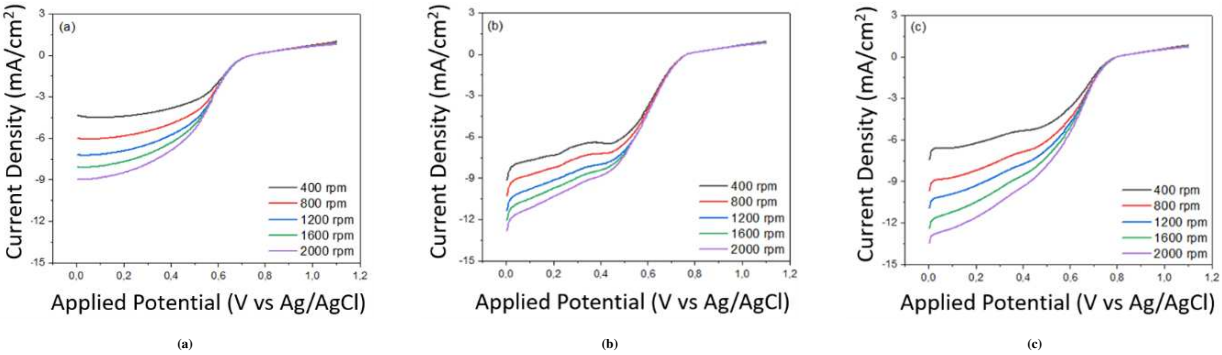

FIGURE 7 Pt/CNT LSV curve with variation pH: (a) pH 9, (b) pH 11, and (c) pH 13

than the lower pH variation sample, yielding 35.64 m2/g at pH 11 and 25.60 m2/g at pH 9. This suggests that the pH variation in sample 13 outperforms the other samples regarding electrochemical performance. This phenomenon is related to particle size, as determined by previous TEM data.

The size of the metal nanoparticles affects the dissolution of the base metal in its support. A more acidic synthesis environment promotes particle agglomeration, which reduces active surface area[18]. Furthermore, there is a potential shift towards a more positive potential at roughly 0.38 V at the peak of Pt-O production and higher pH fluctuations. This can be read as an increase in lipophilicity, the tendency of certain chemical compounds to create oxides by hydrolysis, or the abstraction of oxygen atoms from other molecules, most commonly organic compounds.

This phenomenon can be explained using earlier TEM data on particle size. Whereas prior research indicated that the lipophilicity of Pt particles increases with particle size, our study found that the lipophilicity of Pt particles decreases with particle size. This hypothesis can be investigated further in the electron transfer mechanism passed via the oxygen reduction reaction from the Linear Sweep Voltammetry (LSV) test. A Linear Sweep Voltammetry (LSV) examination of Pt/CNT catalyst specimens was performed to demonstrate the Oxygen Reduction Reaction (ORR) occurrence.

Figure 6 depicts the LSV curves of all three samples. According to the LSV results, the increase in potential onset, which gives potential magnitude at the commencement point of ORR, occurs in tandem with the increase in pH. Whereas pH 13 variation was acquired at 0.798 V, pH 11 variation was produced at 0.764 V, and pH nine variation was obtained at 0.741 V. Furthermore, it is well known that the density of currents that limit diffusion increases as the electrode spins faster and the flow rate increases.

As an example, the LSV curve is displayed at 1600 rpm. Catalyst activity against ORR increases as pH increases during synthesis. When the Pt/CNT catalyst at pH 13 switched to a more positive potential while the Pt/CNT catalyst at pH 11 and pH 9 shifted to a more negative potential sequentially, electrochemical activity decreased in samples with lower pH fluctuations.

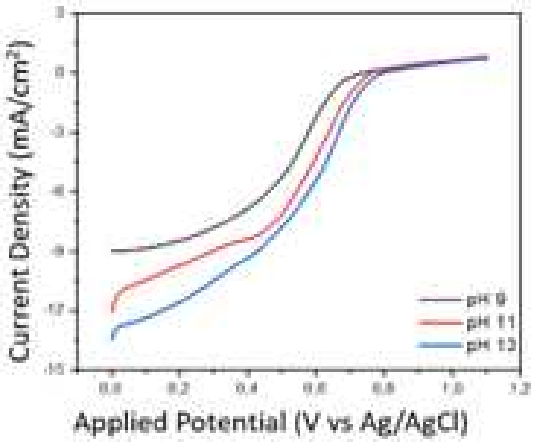

FIGURE 8 LSV curve of Pt/CNT at a constant speed of 1600 rpm with pH variation

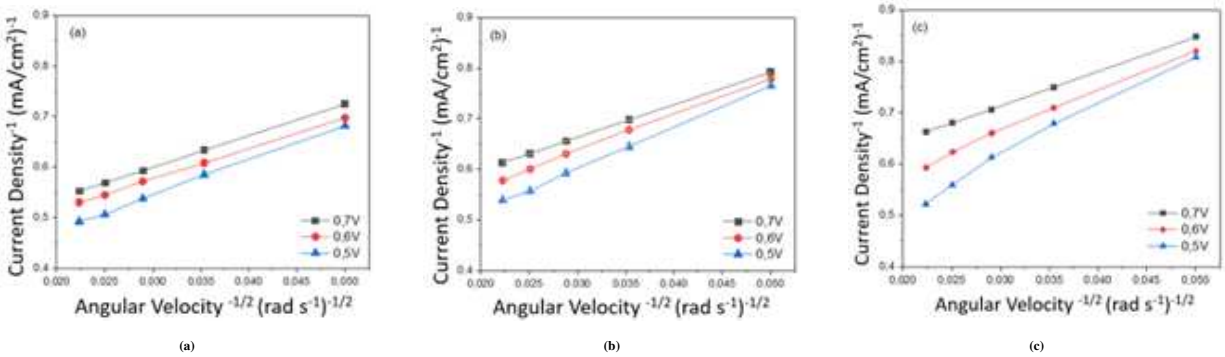

FIGURE 9 Plot the Pt/CNT Kouteck-Levich curve with a variation pH (a) (b) pH 9 (c) pH 11 pH 13

Figure 9 depicts the Kouteck-Levich plot derived from the LSV curve data. Based on the plot gradient, Kouteck-Levich may then be used to compute the number of electrons involved in the ORR. The calculation findings showed that the average number of electrons participating in the reaction with the Pt/CNT catalyst at pH 9 was 3.90, 3.98 at pH 11, and 4.01 at pH 13. This implies that the Pt/CNT catalyst at pH 13 involves the highest electron of 4.01, passing through the ORR's four-electron process.

The four-electron transfer mechanism is preferable in Fuel Cell applications because it is more efficient. The transfer mechanism of two electrons is an incomplete oxygen reduction, which results in low energy conversion efficiency and the creation of hydrogen peroxide. Hydrogen peroxide is a strong oxidant that can destroy electrocatalytic and polymer membrane materials, reducing fuel cell electrochemical performance.

The active surface area of the Pt/CNT catalyst at a higher pH of 13 provides a larger region for electrons to flow during oxygen ORR compared to catalysts at lower pH. Furthermore, these findings support hypotheses from cyclic voltammetry test analyses that reveal a predisposition to oxide production as pH levels decline in synthesis conditions. The data presented and analyzed above demonstrate the optimum catalyst variation pH 13 performance. This information can be used for further research to fabricate one cell of a fuel cell stack.

5 | CONCLUSION

The experiment results and discussions indicate that the Pt/CNT catalyst production utilizing the synthesis method was successful. The effect of pH on the synthesis of Pt/CNT catalysts will affect the crystallinity and shape produced. Whereas rising

pH causes Pt nanoparticles to become more amorphous and the average particle size to decrease due to increased particle dispersion, The results showed that at pH 13, nanoparticles of Pt produced the smallest average particle size of 4,2 nm, followed by 5,1 nm at pH 11, and 7,9 nm at pH 9. At pH 13, the electrochemical performance of the Pt/CNT catalyst performed well. According to the calculations, the catalyst at pH variation 13 has the biggest active surface area of 40.33 m2/g, with a potential onset of 0.798 V involving electrons as much as 4.01 for the oxygen reduction reaction. This is because alkalinity causes the aggregation of nanoparticles in a lower synthesis environment, resulting in a reduction of active surface area.

ACKNOWLEDGMENT

The authors thank PT. Pertamina for financial support of this research collaboration between ITS – PT. Pertamina under-project Fuel Cell Development Using Platinum/Carbon Nano Tubes (CNTs) and Hydrogen Production Development in 2020-2021 with project number No.001/G20420/2020-S0.

CREDIT

Agung Purniawan: Conceptualization, Methodology, Writing - original draft preparation, Formal analysis, Investigation, and Supervision. **Lukman Noerochim:** Conceptualization, Methodology, Writing - original draft preparation, Formal analysis, Investigation, and Supervision. **Sutarsis:** Conceptualization, Methodology, Writing - original draft preparation, and Supervision. **Haryo Satriya Oktaviano:** Conceptualization, Methodology, Writing - original draft preparation, and Supervision. **Hafidz Alim Sukmana:** Funding acquisition. **Muhamad Akbar Wicaksono:** Funding acquisition. **Berlian Aulia Rachman:** Funding acquisition. **Wikan Jatimurti:** Funding acquisition. **Diah Susanti:** Writing - review and editing. **Hanifudin Nurdiansyah:** Resources. **Muhammad Fakhreza Abdul:** Resources.

References

1. Zhuang Y, Zhang S, Yang K, Ren L, Dai K. Antibacterial activity of copper-bearing 316L stainless steel for the prevention of implant-related infection. Journal of Biomedical Materials Research 2019;108(2):484–495. https://onlinelibrary.wiley.com/doi/10.1002/jbm.b.34405.

2. Junping Y, Wei L. Antibacterial 316L Stainless Steel Containing Silver and Niobium. Rare Metal Materials and Engineering 2013;42(10):2004–2008. https://www.sciencedirect.com/science/article/abs/pii/S1875537214600151?via%3Dihub.

3. Goy RC, Morais ST, Assis OB. Evaluation of the antimicrobial activity of chitosan and its quaternized derivative on E. coli and S. aureus growth. Revista Brasileira de Farmacognosia 2016;26(1):122–127. https://www.sciencedirect.com/science/article/pii/S0102695X15002069?via%3Dihub.

4. Rau JV, Fosca M, Graziani V, Egorov AA, Zobkov YV, Fedotov AY, et al. Silver-Doped Calcium Phosphate Bone Cement with Antibacterial Properties. Journal of Functional Biomaterials 2016;7(2):1–10. https://www.mdpi.com/2079-4983/7/2/10.

5. Wei H, Eilers H. From silver nanoparticles to thin films: Evolution of microstructure and electrical conduction on glass substrates. Journal of Physics and Chemistry of Solids 2009;70(2):459–465. https://doi.org/10.1016/j.jpcs.2008.11.012.

6. Kim KM, Son JH, Kim SK, Weller CL, Hanna MA. rom silver nanoparticles to thin films: Evolution of microstructure and electrical conduction on glass substrates. the Institute of Food Technologists 2006;71(3):E119–E124. https://ift.onlinelibrary.wiley.com/doi/10.1111/j.1365-2621.2006.tb15624.x.

7. Nunthanid J, Puttipipatkhachorn A, andGarnet E Peck KY. Physical Properties and Molecular Behavior of Chitosan Films. Drug Development and Industrial Pharmacy 2001;27(2):143–157. https://www.tandfonline.com/doi/full/10.1081/DDC-100000481.

8. Park S, Marsh K, Rhim J. Characteristics of Different Molecular Weight Chitosan Films Affected by the Type of Organic Solvents. the Institute of Food Technologists 2001;67(1):194–197. https://ift.onlinelibrary.wiley.com/doi/10.1111/j.1365-2621.2002.tb11382.x.

9. Godeau XY, Andrianandrasana FJ, Volkova O, Szczepanski CR, Zenerino A, Montreuil O, et al. Chitosan-based hydrogels: From preparation to biomedical applications, Carbohydrate Polymers. International Journal of Biological Macromolecules 2022;199:172–180. https://www.sciencedirect.com/science/article/pii/S0141813021027008?via%3Dihub.

10. Raddaha NS, Cordero-Arias L, Cabanas-Polo S, Virtanen S, Roether JA, Boccaccini AR. Electrophoretic Deposition of Chitosan/h-BN and Chitosan/h-BN/TiO2 Composite Coatings on Stainless Steel (316L) Substrates. Materials 2014;7(3):172–180. https://www.mdpi.com/1996-1944/7/3/1814.

11. Hans M, Támara JC, Mathews S, Bax B, Hegetschweiler A, Kautenburger R, et al. Laser cladding of stainless steel with a copper–silver alloy to generate surfaces of high antimicrobial activity. Applied Surface Science 2014;320:195–199. https://www.sciencedirect.com/science/article/pii/S0169433214020601?via%3Dihub.

12. Pishbin F, Simchi A, Ryan MP, Boccaccini AR. Laser cladding of stainless steel with a copper–silver alloy to generate surfaces of high antimicrobial activity. Surface and Coatings Technology 2011;205(23-24):5260–5268. https://www.sciencedirect.com/science/article/pii/S0257897211005299?via%3Dihub.

How to cite this article: Purniawan A., Noerochim L., Sutarsis S., Oktaviano H.S., Sukmana H.A., Wicaksono M.A., Rachman B.A., Jatimurti W., Susanti D., Nurdiansyah H., Abdul M.F. (2024), Functionalization of Carbon Nanotubes as Support Material of Pt/CNTs Catalyst for Proton-Exchange Membrane fuel Cell, *35(1):60-69*.